Z. Physik 265, 87—104 (1973)


# The ($^2$H—$d$)-Reactions below 200 keV

D. Fick and Ursula Weiss

Max-Planck-Institut für Kernphysik, Heidelberg

Received July 2, 1972

The $^2$H($d$, $n$)- and $^2$H($d$, $p$)-reactions are studied for deuteron energies below 200 keV. It is shown that the $R$-matrix approach of Konopinski and Teller, which is very sensitive to the channel radius used, can be approximated in a way that the dependence on the channel radius does not appear explicitly. This approach appears to be formally equivalent to a kind of "direct approach" of Boersma. This equivalence answers the question why a direct approach to these reactions works at all at low energies. Each reaction is described by three parameters which are determined in a fit to the up to now available data.

## 1. Introduction

The reactions $^2$H($d$, $n$) and $^2$H($d$, $p$) have been investigated since the early days of accelerators in nuclear physics [1, 2]. The first anisotropic angular distribution in nuclear reactions was observed in the $^2$H($d$, $p$)-reaction [3], leading to the prediction of $LS$-coupling [4]. It was just this observation which lead to the prediction of polarization phenomena in nuclear reactions [5]. Naturally these two reactions have been the objects for theoretical studies of nuclear reaction phenomena from the very beginning [4, 6, 7]. A long series of experimental and theoretical papers demonstrates the continuous interest in them [8, 9].

Nowadays the experimental research is concentrated on the study of polarization phenomena [10], using mainly polarized ion sources. Within the course of such experiments the importance of the quintet contributions in the $^2$H$-d$ channel was established [11, 12]. In other experiments an anomaly was observed in the excitation function, especially of the tensor analysing power $A_z$ [12, 13, 14].

A great part of the new theoretical work concentrates on the understanding of these reactions within a microscopic nuclear reaction theory [15]. One of the unsolved problems is the explanation of the large difference of the anisotropy of the angular distributions of the $^2$H($d$, $n$)- and $^2$H($d$, $p$)-reactions. The latest attempt attributes this difference to, up to now, unknown levels in $^4$He which have no pure isospin [16] because of Coulomb mixing.

This short review demonstrates the complexity of these two reactions even at the lowest energies. In spite of a very large number of experiments

[8], there is not too much which can be compared directly. Because of the very low energies more or less thick targets have been used in the experiments, ranging from a few keV to a target thickness larger than the range of the bombarding deuterons used. As a consequence the observed quantities are averaged over different energy intervalls in the various experiments.

In order to compare the data of the different experiments a reevaluation was started, taking into account the various target thickness and target materials used in the different experiments. These calculations and the data themselve are presented in Chap. 2. In Chap. 3 a low energy $R$-matrix approach is presented. The results are compared with those of an approach starting with a more direct interpretation [17]. Chap. 4 is devoted to a comparison of the low energy approach to the experimental data. The appendix contains some formulas which are necessary to obtain the results of Chap. 3.

## 2. Collection of the Available Data

### *2.1. Determination of an Averaged Energy*

To compare data, obtained with a thick target with those achieved with thin targets an averaged energy was calculated. After travelling a certain distance $x$ within a target, a particle with primary energy $E_0$ has the energy

$$E(x)=E_0-\int_0^x \frac{dE}{dx'}(E(x'))\,dx'. \tag{2.1}$$

$(dE/dx)$ is the energy loss of the particle [18] which, because of its energy dependence, depends on the travelled distance $x$. In order to get the averaged energy $E_{av}$ for a certain type of reaction $\alpha$, e.g. $^2\mathrm{H}(d,p)$, one has to calculate

$$E_{av}^{\alpha}=\int_0^d p^{\alpha}(E(x))\,E(x)\,dx \Big/ \int_0^d p^{\alpha}(E(x))\,dx.$$

In this equation $d$ means the target thickness and $p^{\alpha}(E(x))$ the probability, that a certain reaction $\alpha$ will take place at a certain energy $E(x)$. Obviously this ansatz assumes that $p^{\alpha}$ depends on $x$ only because of its energy dependence. An additional possibility would be e.g. an angular dependence of $p^{\alpha}$. In order to avoid complicated calculations this possible angular dependence was neglected. Then it is reasonable to assume that $p^{\alpha}(E(x))$ is proportional to the total cross section for the reaction $\alpha$:

$$E_{av}^{\alpha}=\int_0^d \sigma_{\mathrm{tot}}^{\alpha}(E(x))\,E(x)\,dx \Big/ \int_0^d \sigma_{\mathrm{tot}}^{\alpha}(E(x))\,dx.$$

$E(x)$ is calculated with Eq. (2.1). This requires the knowledge of the total cross section $\sigma_{tot}^{\alpha}$ of the reaction $\alpha$ as a function of energy and the stopping power $(dE/dx)$ for the target material used in the experiment as a function of energy. For $\sigma_{tot}^{\alpha}(E)$ the values of Ruby and Crawford [19] had been used. The values of $(dE/dx)$ were obtained from energy loss experiments for protons assuming, that only the proton within the deuteron is responsible for the energy loss [18]

$$\left(\frac{dE}{dx}(E_d)=\frac{dE}{dx}(E_p/2)\right).$$

For the various target materials the data were taken for the energy loss in $D_2O$ from Wenzel and Whaling [20], in $D_2$ from Allison and Warshaw [21] and in Aluminium from Warshaw [22]. The values for the stopping power in Titanium were interpolated with respect to $Z$ from the known stopping power for Cu [22] and Ag [22].

### *2.2. Summary of Available Data*

#### 2.2.1. Total Cross Section Data

Fig. 1 displays the data available for the total cross section for the $^2$H$(d, n)$-reaction. They are taken from the thin gas target measurements of Arnold *et al.* [23], Booth *et al.* [24], McNeill and Keyser [25] and Preston *et al.* [26]. Therefore, the averaging procedure described in Chap. 2.1 was unnecessary. The cross section data of Manley *et al.* [27] are, by a factor up to five, too low and are therefore omitted.

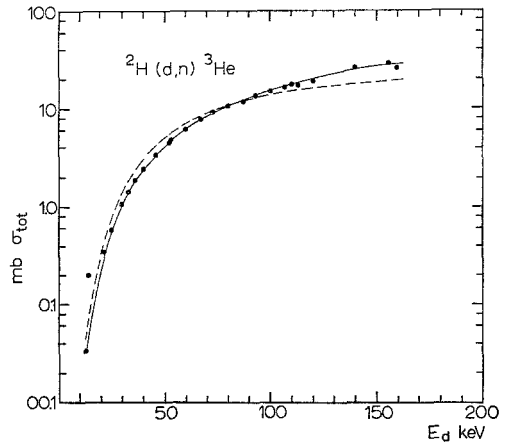


Fig. 1. Total cross section for the $^2$H$(d, n)$-reaction as function of energy. The solid line displays the fit with $l=0$ and 1 contributions, the dashed line with $l=0$ contributions only. For references see Chap. 2.2.1.

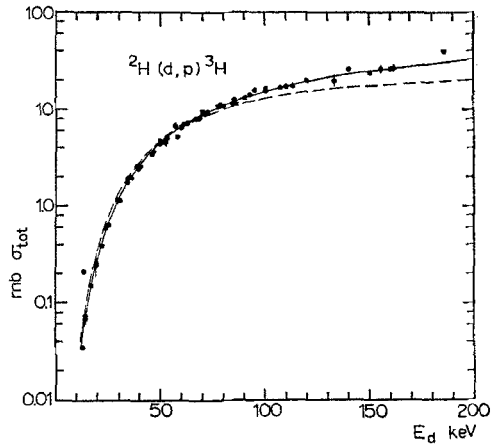


Fig. 2. Total cross section for the $^2H(d,p)$-reaction as function of energy. The solid line displays the fit with $l=0$ and 1 contributions, the dashed line with $l=0$ contributions only. For references see Chap. 2.2.1.

Fig. 2 contains the available data for the total cross section of the $^2H(d,p)$-reaction, taken from Arnold *et al.* [23], Sanders *et al.* [28], Davenport *et al.* [29], Wenzel and Whaling [30], Booth *et al.* [24], McNeill and Keyser [25], Preston *et al.* [26] and Cook and Smith [31]. The data of Wenzel and Whaling [30] were obtained with a thick heavy ice target, for which averaged energies had been assigned by the authors themselve. The cross section data of Cook and Smith [31] were obtained with a thick Zr-D target. Averaged energies had been calculated along the outlines of Chap. 2.1. Taking into account these averaged energies, the data fit very well the general trend of the other data. The cross section data of Bretcher *et al.* [32], obtained with a heavy ice target, are in general much too large. They are far outside the general trend and are not taken into account for the following.

All data points of Figs. 1 and 2 seem to be consistent with each other, except the two values at $E_d = 14$ keV obtained by Arnold *et al.* [23] which are definitely too high in both reactions. They are therefore omitted in the further considerations.

### 2.2.2. The Anisotropy Coefficient

Both reactions, the $^2H(d,n)$ and $^2H(d,p)$, show an anisotropy in their angular distributions down to the lowest energies. For the energies under consideration, it is sufficient to take into account only the term

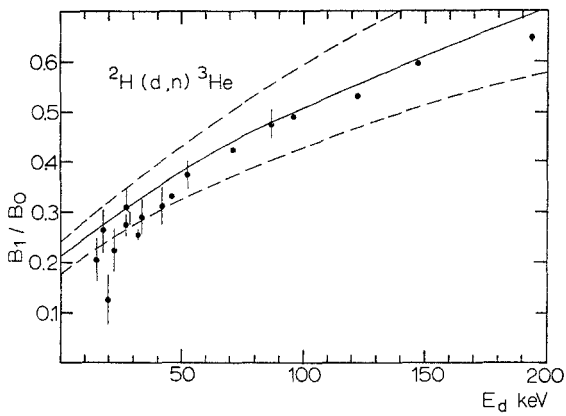


Fig. 3. Excitation function of the anisotropy coefficient $B_1/B_0$ for the $^2$H($d$, $n$)-reaction. The solid line is obtained with the fit parameters of Chap. 4.3, the dashed lines correspond to the maximal errors. For references see Chap. 2.2.2.

with $L_2(\cos\vartheta)$ in a Legendre-polynomial expansion [33]:

$$\sigma(\vartheta, E)=\frac{\lambda^2}{36}\left(B_0(E)+B_1(E)\,L_2(\cos\vartheta)\right). \tag{2.2}$$

The ratio $(B_1/B_0)$ is called anisotropy coefficient. In some papers the angular distributions are expanded in terms of $(\cos\vartheta)^{2n}$:

$$\sigma(\vartheta, E)\propto 1+A\cos^2\vartheta.$$

Then the relation

$$B_1/B_0=2A/(3+A)$$

holds between the anisotropy coefficient $(B_1/B_0)$ and $A$.

In Fig. 3 the excitation function of the anisotropy coefficient is displayed. The values are taken from Theus *et al.* [34], Eliot *et al.* [35] and Booth *et al.* [24]. In Fig. 4 the same quantity is shown for the $^2$H($d$, $p$)-reaction, containing the data of Davenport *et al.* [29], Theus *et al.* [34], Booth *et al.* [24] and Tai *et al.* [36], who all used thin gas targets in their experiments. Fig. 4 also contains the values of Bretcher *et al.* [32], which were obtained with a thick heavy ice target. For these data points averaged energies have been calculated. The data points of Eliot *et al.* [35], Manning *et al.* [37] and Timm *et al.* [38] have been omitted, either because of their large error bars or because they are too far away from the general trend of the other data points.

There exist two measurements which are concerned with the anomaly around 100 keV [12, 39]. They are not included in Fig. 4 and the further

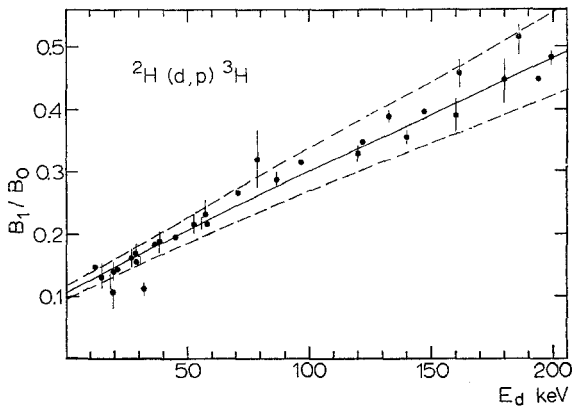


Fig. 4. Excitation function of the anisotropy coefficient $B_1/B_0$ for the $^2$H$(d, p)$-reaction. The solid line is obtained with the fit parameters of Chap. 4.3, the dashed lines correspond to the maximal errors. For references see Chap. 2.2.2.

considerations because the following interpretation is devoted only to the smooth behaviour of the two reactions. These two measurements will be discussed in another paper [40], together with the corresponding polarization measurements. For this reason also the other existing polarization measurements are not considered in the following.

### 2.2.3. Ratio of the Total Cross Section

The data for the ratio of the total cross sections of the neutron and proton channel $\sigma^n_{tot}/\sigma^p_{tot}$ are not measured directly by the various authors but calculated from the anisotropy factors determined in their experiment. Therefore, the data obtained in the various experiments are very difficult to compare because they exhibit very large deviation from each other. Therefore, Fig. 5 contains only the data from Theus *et al.* [34]. The values of McNeill and Keyser [25], Eliot *et al.* [35] and Booth *et al.* [24] and the data reevaluated by McNeill [41] were not taken into account for the above reasons.

### 2.2.4. Ratio of the Cross Sections at 90°

This ratio can be determined directly from the experiment. Fig. 6 displays the data available for $\sigma_n(90°)/\sigma_p(90°)$ taken from Theus *et al.* [34], Eliot *et al.* [35], and the values of Arnold *et al.* [23], corrected by McNeill [41]. The data of Booth *et al.* [24] and McNeill and Keyser [25] were omitted because of their large error bars.

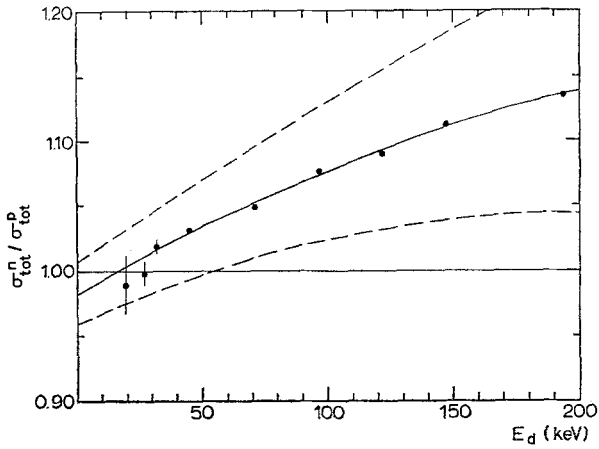


Fig. 5. Ratio of total cross sections of the neutron and proton channel as function of energy. The solid line is obtained with the fit parameters of Chap. 4.2, the dashed lines correspond to the maximal errors. For references see Chap. 2.2.3.

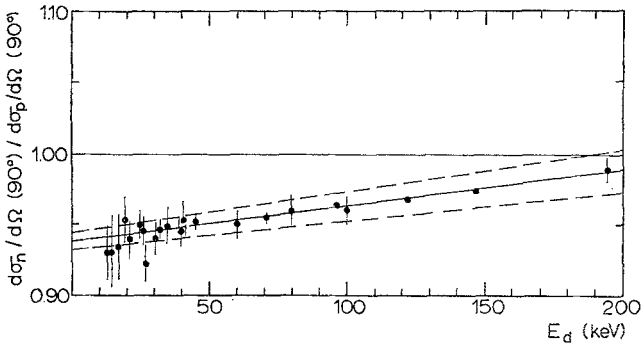


Fig. 6. Ratio of cross section of the neutron and proton channel at 90° as function of energy. The solid line is obtained with the fit parameters of Chap. 4.2, the dashed lines correspond to the maximal errors. For references see Chap. 2.2.4.

## 3. The Low Energy Limit (Theory)

The classical approach concerning the $^2$H($d$, $n$)- and $^2$H($d$, $p$)-reactions had been given by Konopinski and Teller [4] and by Beiduk *et al.* [7]. The basic idea of these papers is the assumption that the only energy dependence of the observables is given by the appropriate barrier penetration factors $P_l$ in the $^2$H—$d$ channel. (This approach is later called a $R$-matrix approach for obvious reasons.) This assumption is plausible for low deuteron energies, considering the high $Q$-value of the reactions

(3.3 and 4.1 MeV respectively) and the smooth behaviour of the $n-{}^3\mathrm{He}$ and $p-{}^3\mathrm{H}$ scattering at the relevant energies [8]. Within this approach, one is left with the "intrinsic reaction probabilities" which should be independent of energy.

One of the severe objections [17] to the approach of Beiduk *et al.* [7] is the fact, that the calculated values of the penetration factors depend strongly on the boundary conditions (hard sphere, black nucleus) and the interaction radius $R$ used. Konopinski and Teller [4] found an interaction radius of $R=7$ fm to be appropriate for a description of the data. In order to avoid these ambiguities Boersma [17] proposed another low energy approach, based on some kind of DWBA treatment of the two reactions. An analogous idea was also tried by Duder *et al.* [42] and Yu [43]. In any case, it is difficult to understand, why a DWBA-ansatz can work at these low energies where the angular momentum are restricted to the lowest ones.

It is the purpose of the following considerations to show

(i) that only the boundary condition of a black nucleus is able to reproduce the data.

(ii) that there is really no specific interaction radius $R$, e.g. $R=7$ fm which describes the data better than another interaction radius.

(iii) that the DWBA approach is formally identical at low energies with the approach of Beiduk *et al.* [7], using the boundary condition of a black nucleus.

(iv) that, as a consequence of (iii) the approach of Beiduk *et al.* [7] yields at the low energies a $R$-independent analysis of the data.

### *3.1. The R-Matrix Approach*

According to the approach of Beiduk *et al.* [7] and the angular momentum decomposition of Rook and Goldfarb [33] the coefficients $B_0$ and $B_1$ of Eq. (2.2) can be expanded as:

$$\sigma_{\mathrm{tot}}=\frac{4\pi}{36k_{\mathrm{in}}^2}B_0=c_0P_{l=0}(k,R)+c_1P_{l=1}(k,R), \tag{3.1}$$

$$\tilde{B}_1=\frac{1}{36k_{\mathrm{in}}^2}B_1=c_1'P_{l=1}(k,R). \tag{3.2}$$

In this expansion the $l=2$ matrix elements have been neglected because of the low energies involved.

The penetration factors $P_l$ are determined by the regular and irregular Coulomb functions $F_l$ and $G_l$ [44]. With the boundary condition of a black nucleus, which is usual in the $R$-matrix theory [45], one gets

$$P_l=\rho/\left(F_l^2(k,R)+G_l^2(k,R)\right) \tag{3.3}$$

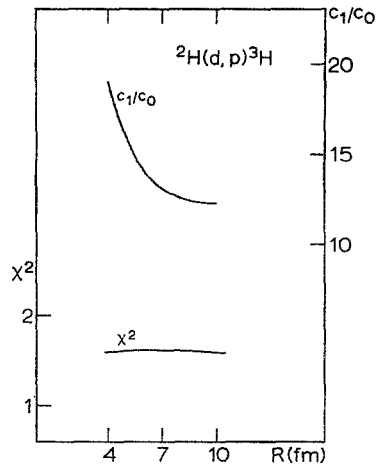


Fig. 7. $\chi^2$ and the ratio $c_1/c_0$ as function of the channel radius $R$ for a $R$-matrix fit of the $^2$H$(d, p)$-reaction. For details see Chap. 3.1.

and for the boundary condition of a hard sphere [46]

$$P_l = F_l^2(k, R)/(F_l^2(k, R) + G_l^2(k, R)). \tag{3.4}$$

In the first instance the excitation function of the total cross section (Figs. 1 and 2) were fitted with the ansatz of Eq. (3.1) and energy independent coefficients $c_0$ and $c_1$. Using the common boundary condition of a black nucleus (Eq. (3.3)) one gets excellent fits to the total cross section (solid lines in Figs. 1 and 2). It is impossible to get the correct trend if one assumes only $l=0$ contributions to the total cross section (dashed lines in Figs. 1 and 2). This again proves the importance of the $l=1$ contributions in these two reactions. A variation of the channel radius between 4 and 10 fm does not change the $\chi^2$ of the fit at all. But the ratio of $c_1/c_0$, which corresponds to the ratio of $l=1$ to $l=0$ contributions, is changed very drastically. As an example Fig. 7 displays for the $^2$H$(d, p)$-reaction the obtained $\chi^2$ and ratio $c_1/c_0$ as a function of the channel radius $R$. Fig. 7 demonstrates, that the fit is really independent of the channel radius $R$, as it is expected in a $R$-matrix approach. This means that the channel radius of 7 fm, which has been used since the early paper of Konopinski and Teller [4] as the appropriate radius is rather meaningless. On the other hand, such a fit shows that the ratio $c_1/c_0$ depends strongly on the channel radius and is therefore not accessible to a direct and naive interpretation.

Next a fit with the boundary condition of a hard sphere (Eq. (3.4)) was tried. Negative values of $c_1$ were always obtained, independent of the

channel radius $R$ used. On the other hand it is obvious, that $c_1$ must be positive, because a total cross section is always a sum of absolute values of matrix elements, with positive numbers in front [33]. In this way one can rule out this boundary condition as physical meaningless.

### *3.2. Low Energy Limit of Penetration Factors and of the R-matrix Approach*

It is the purpose of the following considerations to get a parametrisation of the cross section data within the framework of a $R$-matrix approach, which does not depend explicitly on the channel radius $R$. This has the advantage that the parameters extracted from the experimental data are, in this sense, model independent. They can be determined in a unique way and are accessible to a naive and direct interpretation.

For the Coulomb wave function the nomenclature of Abramowitz and Stegum [44] is used throughout. The Coulomb wavefunction depends on the two variables $\eta$ and $\rho$. For the *d-d* system one gets $\eta=\sqrt{0.05/E}$ and $\rho\approx 0.55\sqrt{E}$ with the laboratory energy $E$ in MeV. For deuteron energies between 0 and 0.2 MeV $\eta$ ranges between $\infty$ and 0.5 and $\rho$ between 0 and 0.25. For this range of $\eta$ and $\rho$, $F_l^2$ is always much smaller than $G_l^2$. (For the *d-d* system one finds that $(F_l/G_l)^2 \leqq 2\cdot 10^{-5}$ for $E\leqq 0.2$ MeV!!). Therefore the penetration factor $P_l$ (Eq. (3.3)) can be written as

$$P_l=\rho/G_l^2.$$

With this approximation the following expression for the penetration factors is obtained, as shown in Appendix A:

$$P_l=g_l^{-2}(2l+1)^2\,C_l^2(\eta)\,\rho^{2l+1} \tag{3.5}$$

$$g_l \begin{cases} =0.7 & \text{for } l=0 \\ =1 & \text{for } l>0 \end{cases} \text{ and independent of energy!}$$

and

$$C_0^2(\eta)=2\pi\eta/(\exp(2\pi\eta)-1).$$

The penetration factors of the exit channel are now taken into account in the $R$-matrix approach in order to compare later correctly with the DWBA approach. Because of the large $Q$-values one has to consider the penetration factors for large $\rho$ and small $\eta$. It is wellknown [44], that for these limits

$$F_l^2+G_l^2\to 1$$

and therefore

$$P_l^{\text{fin}}\to\rho^{\text{fin}}.$$

Using this relation with Eqs. (2.2), (3.1) and (3.2), one obtains the differential cross section as:

$$\begin{aligned}\sigma &= \frac{1}{36\,k_{\text{in}}^2}\left(B_0 + B_1\,L_2(\cos\vartheta)\right)\\ &= \frac{1}{36}\,\frac{\rho_{\text{fin}}}{k_{\text{in}}^2}\left(a_0\,P_{l=0} + a_1\,P_{l=1} + b P_{l=1}\,L_2(\cos\vartheta)\right).\end{aligned} \tag{3.6}$$

With the use of Eq. (3.5) one gets for the ratio of $P_{l=1}/P_{l=0}$

$$(P_{l=1}/P_{l=0}) = g_0^2(1+\eta^2)\,\rho_{\text{in}}^2$$

and for $P_{l=0}$

$$P_{l=0} = g_0^{-2}\,C_0^2(\eta)\,\rho_{\text{in}}.$$

With Eq. (3.6) and remembering that $\rho\eta$ is independent of the energy and $\eta^2 = 0.05/E$ one finds the following cross section:

$$\begin{aligned}\sigma &= \frac{k_{\text{fin}}}{k_{\text{in}}}\,C_0^2(\eta)\,a(1+\alpha\varepsilon)\left(1+\frac{\beta\varepsilon}{1+\alpha\varepsilon}\,L_2(\cos\vartheta)\right)\\ &= \frac{1}{4\pi}\,\sigma_{\text{tot}}\left(1+\frac{B_1}{B_0}\,L_2(\cos\vartheta)\right)\end{aligned} \tag{3.7}$$

where $\varepsilon = E + 0.05$ with $E$ in MeV.

The definition of the coefficients $\alpha$ and $\beta$ is chosen formally in the same way as it was done in the DWBA approach of Boersma [17] in order to demonstrate the formal equivalence of the low energy $R$-matrix and DWBA approach. The coefficients $a$, $\alpha$ and $\beta$ now contain all the energy independent parts of the cross section. They include also all the terms which depend formally on the channel radius $R$. These coefficients are taken now as free parameters. It is obvious that a channel radius independent parametrisation of the $R$-matrix approach is achieved in this way.

By way of comparison one gets for the individual parts of the cross section in Eq. (3.7)

$$\sigma_{\text{tot}}\Big/\left(\frac{k_{\text{fin}}}{k_{\text{in}}}\right)C_0^2(\eta) = 4\pi a(1+\alpha\varepsilon) \tag{3.8}$$

and

$$(B_1/B_0) = \beta\varepsilon/(1+\alpha\varepsilon). \tag{3.9}$$

A discussion of these results should include the following remarks:

(i) One needs three energy independent parameters to describe the $^2$H($d$, $n$)- and $^2$H($d$, $p$)-reaction at low energies if this approach is to be able to fit the data. This is to be expected, because it was demonstrated

in the beginning of this chapter that the full $R$-matrix approach provides an excellent fit of the data.

(ii) this approach produces formally the same equations as a DWBA treatment of the reactions [17]. This shows why a DWBA approach [17, 42, 43] works even at these very low energies.

(iii) if the bombarding energy goes to zero, the anisotropy coefficient approachs a nonzero value

$$E \to 0; \quad (B_1/B_0) \to 0.05\,\beta/(1+0.05\,\alpha).$$

This means that as long as $\beta=0$ or as long as one has at energies unequal to zero $l=1$ contributions to the cross section, the anisotropy coefficient $B_1/B_0$ is unequal to zero also for $E=0$. This fact already has been mentioned by Konopinski and Teller [4] and by Boersma [17] in his DWBA approach.

## 4. Comparison with the Data

As shown in Chap. 3 each reaction can be described in the low energy limit by three parameters $a$, $\alpha$ and $\beta$ (Eqs. (3.8) and (3.9)). In order to get these parameters Eqs. (3.8) and (3.9) were fitted to the experimental data which has been gathered in Chap. 2.

4.1. In order to compare the data for the total cross section with Eq. (3.8) it is more instructive to plot first

$$\sigma_{\text{tot}} \Big/ \left(\frac{k_{\text{fin}}}{k_{\text{in}}}\right) C_0^2(\eta) = 4\pi a(1+\alpha\varepsilon) \tag{4.1}$$

as a function of the deuteron energy. Figs. 8 and 9 display this quantity for the $^2\text{H}(d, n)$- and $^2\text{H}(d, p)$-reactions. It is obvious that any accuracy of the experimental points which might be inferred from the logarithmic plots of the cross section in Figs. 1 and 2 has disappeared. In addition it is clear, that from these data the coefficient $\alpha$ in Eq. (4.1) can only determined with very poor accuracy.

A least square fit of the data in Figs. 8 and 9 with Eq. (4.1) yields

$$a^n = 1.2 \pm 0.1 \quad \text{and} \quad a^p = 2.2 \pm 0.1$$

and $\alpha^n \approx 5$, $\alpha^p \approx 2$ with very large error bars.

Next the anisotropy coefficient

$$(B_1/B_0) = \beta\varepsilon/(1+\alpha\varepsilon)$$

was fitted to the data of Figs. 3 and 4. Because in the proton channel the coefficient $\alpha^p$ is rather small, it is difficult to determine. This leads to a

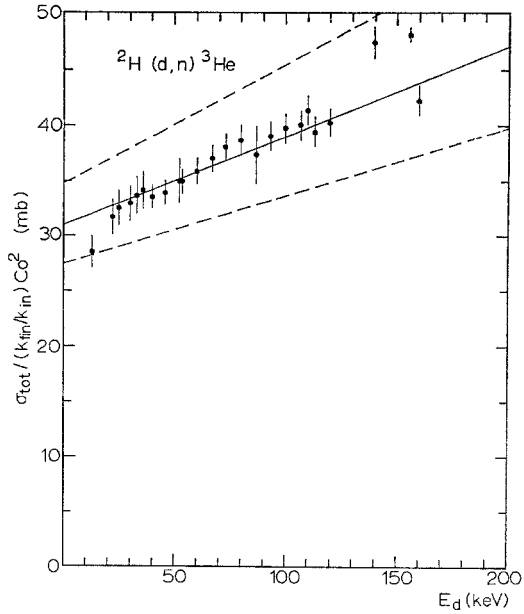


Fig. 8. $\sigma_{tot}/(k_{fin}/k_{in})\,C_0^2$ as function of energy for the $^2$H$(d, n)$-reaction. The solid line is obtained with the fit parameters of Chap. 4.3., the dashed lines correspond to the maximal errors

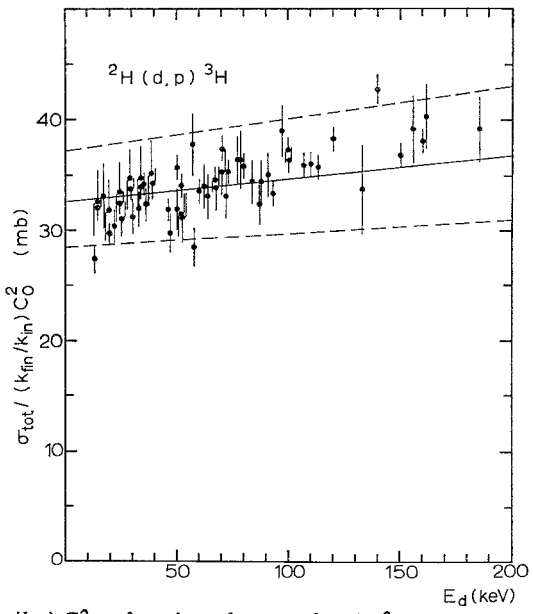


Fig. 9. $\sigma_{tot}/(k_{fin}/k_{in})\,C_0^2$ as function of energy for the $^2$H$(d, p)$-reaction. The solid line is obtained with the fit parameters of Chap. 4.3., the dashed lines correspond to the maximal errors

rather large error bar for this parameter. From the least square fit the following parameters were obtained:

$$\beta^n = 4.9 \pm 0.2, \quad \alpha^n = 3.2 \pm 0.3 \quad \text{and} \quad \beta^p = 2.2 \pm 0.1, \quad \alpha^p = 0.7 \pm 0.2.$$

4.2. In order to get a check of these fits and to obtain a real estimate of the error bars, which are certainly too small, one can use the known ratios of $\sigma^n/\sigma^p$ and $\sigma^n(90°)/\sigma^p(90°)$ which are displayed in the Figs. 5 and 6. For an independent check the ratio $\sigma^n_{\text{tot}}/\sigma^n_{\text{tot}}$ must be used with caution because it is not measured directly but computed from known anisotropy coefficients. Using the Eqs. (3.8) and (3.9) one gets the following expressions for these two ratios [17]:

$$\begin{aligned}
\sigma^n_{\text{tot}}/\sigma^p_{\text{tot}} &= \kappa\gamma(1+\alpha^n\varepsilon)/(1+\alpha^p\varepsilon) \\
&\approx \kappa\gamma\{1+(\alpha^n-\alpha^p)\varepsilon-(\alpha^n-\alpha^p)\alpha^p\varepsilon^2) \\
\sigma^n(90°)/\sigma^p(90°) &= \kappa\gamma\{1+(\alpha^n-\tfrac{1}{2}\beta^n)\varepsilon\}/\{1+(\alpha^p-\tfrac{1}{2}\beta^p)\varepsilon\} \\
&\approx \kappa\gamma\{1+[(\alpha^n-\alpha^p)-\tfrac{1}{2}(\beta^n-\beta^p)]\varepsilon\}
\end{aligned}$$

with $\gamma = (a^n/a^p)$ and $\kappa = k^n_{\text{fin}}/k^p_{\text{fin}}$.

For $\sigma^n(90°)/\sigma^p(90°)$ only the linear term in the expansion was taken into account because this ratio shows experimentally no significant deviation from a straight line (Fig. 5).

A least square fit to the data yields the following results:

$$\begin{aligned}
\sigma^n_{\text{tot}}/\sigma^p_{\text{tot}}&: \gamma = 1.026 \pm 0.013, \quad (\alpha^n-\alpha^p) = 1.4 \pm 0.2 \\
&\qquad\qquad (\alpha^n-\alpha^p)\alpha^p = 1.7 \pm 0.6 \\
\sigma^n(90°)/\sigma^p(90°)&: \gamma = 1.028 \pm 0.006, \\
(\alpha^n-\alpha^p)-\tfrac{1}{2}(\beta^n-\beta^p) &= 0.272 \pm 0.033.
\end{aligned}$$

The solid and dashed lines in the Figs. 5 and 6 display the result of the fits including the errors. It should be pointed out that for $\sigma^n/\sigma^p$ the terms proportional to $\varepsilon$ and $\varepsilon^2$ can be determined only with a large error because there are not enough data to determine the two parameters independently with a good accuracy. For this reason, in spite of a rather perfect fit to the data points (solid line in Fig. 5), the errors are so large (dashed lines in Fig. 5).

4.3. At the end of this procedure it was attempted to find a set of parameters $a$, $\alpha$ and $\beta$ which are consistent with the results of Chap. 4.2

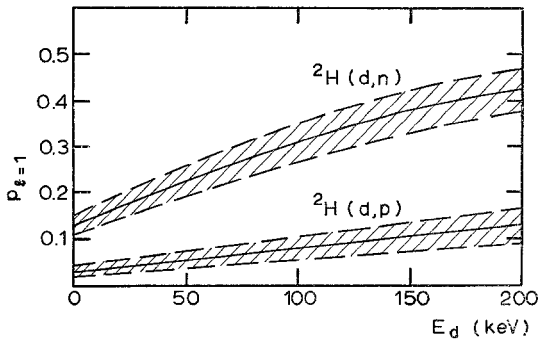


Fig. 10. Fraction $p_{l=1}$ of $l=1$ contributions to the total cross section as function of energy for the $^2$H($d$, $n$)- and $^2$H($d$, $p$)-reaction, calculated with the fit parameters obtained in Chap. 4.3.

and which have the appropriate errors. The following set was found:

$$\begin{aligned} a^n &= 2.1 \pm 0.2 \quad & a^p &= 2.5 \pm 0.3 \\ \alpha^n &= 3.0 \pm 0.6 \quad & \alpha^p &= 0.6 \pm 0.2 \\ \beta^n &= 4.9 \pm 0.5 \quad & \beta^p &= 2.2 \pm 0.2. \end{aligned} \tag{4.2}$$

The solid lines and the errors in the Figs. 1 to 4 which display $\sigma_{\text{tot}}$ and $(B_1/B_0)$ for both reactions had been calculated using these values. It is obvious that the error bars, especially for the neutron channel, are a little bit too large. But these large error bars are necessary to provide agreement with the results of the fits for $\sigma^n_{\text{tot}}/\sigma^p_{\text{tot}}$ and $\sigma^n(90°)/\sigma^p(90°)$ also.

These results may be compared with those of Boersma [17], who determined $\alpha$ and $\beta$ only. While the values for the proton channel agree completely, there is a slight difference in the neutron channel (Boersma: $\alpha^n=1.9$, $\beta^n=4.2$). This difference may be attributed to the fact that Boersma has determined his parameters essentially from the ratio $\sigma^n_{\text{tot}}/\sigma^p_{\text{tot}}$. As pointed out before the fit for $\sigma^n_{\text{tot}}/\sigma^p_{\text{tot}}$ is ambiguous.

4.4. In a last point one may ask for the relative $l=1$ contributions $p_{l=1}$ to the cross section for the two reactions. This contribution is given by

$$p_{l=1} = \alpha\varepsilon/(1+\alpha\varepsilon)$$

and plotted against the deuteron energy for both reactions in Fig. 10. The $l=1$ contributions in the $^2$H($d$, $n$)-reaction are larger by a factor of 4 to 6 than these of the $^2$H($d$, $p$)-reaction. It is not clear if this has anything to do with the structure of the $^4$He-compound system which, in this energy region, influences just the $l=1$ and not the $l=0$ contributions. One indication in this possibility may be the fact that the ratio for the $l=0$ contributions, which is given by $a^n/a^p$, was found to be one within the

error bars. On the other hand, there is some speculation which attributes this difference to a isospin impurity resulting from Coulomb mixing [16].

The authors are indebted to Stud.-Rat H. Mendel for the computer code used in Chap. 3.1 and to Stud.-Rat H. J. Thiemann who helped to collect the data and to calculate the averaged energies. Prof. H. A. Weidenmüller and Dr. H. M. Hofmann contributed with helpful discussions.

## Appendix A

In order to get an approximation for the penetration factors $P_l$, valid for large $\eta$ and small $\rho$, one can start with an approximation for the irregular Coulomb functions $G_0$ given by Jackson and Blatt [47] valid for small $\rho$ ($\rho \ll 1$):

$$G_0 \approx C_0^{-1}(\eta)[1+2\eta\rho(\ln 2\eta\rho+2\gamma-1)+2\eta\rho\, h(\eta)+\cdots] \quad \text{(A.1)}$$

with $\gamma=0.5772$ the Euler Constant and

$$h(\eta)=\eta^2\Big/\left(\sum_{k=1}^{\infty} k(k^2+\eta^2)\right)-\ln\eta-\gamma.$$

Because $\eta\rho$ is independent of energy (for $^2\mathrm{H}-d$ system $\eta\rho\approx 0.12$) one notices that in Eq. (A.1), within the rectangular bracket only $2\eta\rho h(\eta)$ depends on the energy. Inserting the proper values for the $d$-$d$ system one finds:

$$G_0 \approx C_0^{-1}(\eta)[1-0.3+2\eta\rho\, h(\eta)+\cdots]. \quad \text{(A.2)}$$

Following Jackson and Blatt [47] and Abramowitz and Stegum [44] one gets for $h(\eta)$ the following expansion useful for large values of $\eta$:

$$h(\eta)=\mathrm{Re}\,\Psi(1+i\eta)-\ln\eta\approx\ln\eta+\sum_{n=1}^{\infty}\frac{(-1)^{n-1}B_{2n}}{2n\eta^{2n}}-\ln\eta$$

where $\Psi(1+i\eta)$ is the complex $\Psi$-function, defined by Abramowitz and Stegum [44] and $B_{2n}$ are the wellknown Bernoulli-numbers [44]. In this way one finds for the function $h(\eta)$:

$$h(\eta)\approx\frac{1}{12\eta^2}+\frac{1}{120\eta^4}+\frac{1}{252\eta^6}+\cdots.$$

Inserting this equation into Eq. (A.2) and remembering that $\eta^2=0.05/E$ one gets for the irregular Coulombfunction

$$G_0 \approx C_0^{-1}(\eta)(1-0.3+0.4E+0.8E^2+\cdots).$$

Up to $E\approx 0.2$ MeV the energy dependent parts are smaller than approximately 10%. If they are neglected one gets the following simple expression for $G_0$:

$$G_0 \approx g_0/C_0(\eta) \quad \text{with } g_0=0.7.$$

For the calculation of the $G_l$ with $l\geqq 1$ one uses the Wronskian relation

for the Coulomb functions [43]:

$$F_{l-1}\,G_l - F_l\,G_{l-1} = l/\sqrt{l^2+\eta^2}.$$

Taking into account that for $E_d \leqq 0.2$ MeV $\rho \leqq 0.1$, one neglects in an expansion of $F_0$ and $F_1$ terms higher than the lowest power in $\rho$ (which is $\rho^{l+1}$). Than one gets for $F_l$

$$F_l = C_l(\eta)\,\rho^{l+1}.$$

The higher terms are always smaller than $10^{-2}$ in the energy region under consideration.

With

$$C_l(\eta) = C_{l-1}(\eta)\sqrt{l^2+\eta^2}/l(2l+1)$$

one gets for $G_l$

$$G_l = g_l/[(2l+1)\,C_l\,\rho^l]$$

with $g_0 = 0.7$ and $g_l = 1$ for $l \geqq 1$.

With the last relation the penetration factors in this approximation are found to be

$$P_l = g_l^{-2}(2l+1)^2\,C_l^2(\eta)\,\rho^{2l+1}.$$

## References


1. Lawrence, E. O., Livingstone, M. S., Lewis, G. N.: Phys. Rev. **44**, 56 (1933)
2. Oliphant, M. L. E., Harteck, P., Rutherford, L.: Proc. Roy. Soc. (London), Ser. A **144**, 692 (1934)
3. Kempton, A. E., Browne, B. C., Maasdorp, R.: Proc. Roy. Soc. (London), Ser. A **157**, 386 (1936)
4. Konopinski, E. J., Teller, E.: Phys. Rev. **73**, 822 (1948)
5. Wolfenstein, L.: Phys. Rev. **75**, 342 (1949)
6. Schiff, L.: Phys. Rev. **51**, 783 (1937)
   Flügge, S.: Z. Physik **108**, 545 (1938)
7. Beiduk, F. M., Pruett, J. R., Konopinski, E. J.: Phys. Rev. **77**, 622 (1950)
   Pruett, J. R., Beiduk, F. M., Konopinski, E. J.: Phys. Rev. **77**, 628 (1950)
8. Meyerhof, W. E., Tombrello, T. A.: Nucl. Phys. A **109**, 1 (1968)
9. Fairmann, S., Meyerhof, W. E.: Nucl. Phys. to be published
10. Proceedings of the Third International Symposium on Polarization Phenomena in Nuclear Reactions, Eds. Barshall, H. H., Haeberli, W. University of Wisconsin Press 1971
11. Petitjean, C., Huber, P., Paetz gen. Schieck, H., Striebel, H. R.: Helv. Phys. Acta **40**, 401 (1967)
    Paetz gen. Schieck, H., Huber, P., Petitjean, C., Rudin, H., Striebel, H. R.: Helv. Phys. Acta **40**, 414 (1967)
12. Franz, H. W., Fick, D.: Nucl. Phys. A **122**, 591 (1968)
    Fick, D., Franz, H. W.: Phys. Lett. **27** B, 541 (1968)
13. Fick, D.: Z. Physik **221**, 451 (1969)
14. Kilian, K., Fritz, J., Gückel, F. A., Kankowsky, R., Neufert, A., Niewisch, J., Fick, D.: Proceedings of the International Conference on Few Particle Problems in the Nuclear Interaction, Los Angeles, 667 (1972)
15. Hackenbroich, H. H., Heiss, P., Stöwe, H.: Proceedings of the International Conference on Few Particle Problems in the Nuclear Interaction, Los Angeles, 1972

16. Sergeyev, V. A.: Phys. Lett. **38** B, 286 (1972)
17. Boersma, H. J.: Nucl. Phys. A **135**, 609 (1969)
18. Whaling, W.: Handbuch der Physik, Band XXXIV, S. 193, Berlin-Göttingen-Heidelberg: Springer 1958
19. Ruby, L., Crawford, R. B.: Nucl. Instr. Methods **24**, 413 (1963)
20. Wenzel, W. A., Whaling, W.: Phys. Rev. **85**, 499 (1952)
21. Allison, S. K., Warshaw, S. D.: Rev. Mod. Phys. **25**, 779 (1953)
22. Warshaw, S. D.: Phys. Rev. **76**, 1759 (1949)
23. Arnold, W. R., Phillips, J. A., Sawyer, G. A., Stovall, E. J., Tuck, J. L.: Phys. Rev. **93**, 483 (1954)
24. Booth, D. L., Preston, G. R., Shaw, P. F. D.: Proc. Phys. Soc. (London) A **69**, 265 (1956)
25. McNeill, K. G., Keyser, G. M.: Phys. Rev. **81**, 602 (1951)
26. Preston, G. R., Shaw, P. F. D., Young, S. A.: Proc. Roy. Soc. (London), Ser. A **226**, 206 (1954)
27. Manley, J. H., Coon, J. H., Graves, E. R.: Phys. Rev. **70**, 101 (1946)
28. Sanders, J. H., Moffatt, J., Roaf, D.: Phys. Rev. **77**, 754 (1950)
Moffatt, J., Roaf, D., Sanders, J. H.: Proc. Roy. Soc. (London), Ser. A **212**, 220 (1952)
29. Davenport, P. A., Jeffries, J. O., Owen, M. E., Price, F. V., Roaf, D.: Proc. Roy. Soc. (London), Ser. A **216**, 66 (1953)
30. Wenzel, W. A., Whaling, W.: Phys. Rev. **88**, 1149 (1952)
31. Cook, C. F., Smith, J. R.: Phys. Rev. **89**, 785 (1953)
32. Bretscher, E., French, A. P., Seidl, F. G. P.: Phys. Rev. **73**, 815 (1948)
33. Rook, J. R., Goldfarb, L. J. B.: Nucl. Phys. **27**, 79 (1961)
34. Theus, R. B., McGarry, W. I., Beach, L. A.: Nucl. Phys. **80**, 273 (1966)
Theus, R. B., McGarry, W. I., Beach, L. A.: Phys. Rev. Letters **14**, 232 (1965)
35. Eliot, E. A., Roaf, D., Shaw, P. F. D.: Proc. Roy. Soc. (London), Ser. A **216**, 57 (1953)
36. Tai, Y. K., Hsu, Y. C.: Nucl. Phys. **46**, 153 (1963)
37. Manning, H. P., Huntoon, R. D., Myers, F., Young, V.: Phys. Rev. **61**, 371 (1942)
38. Timm, U., Neuert, H., Elsner, B.: Z. Physik **139**, 425 (1954)
39. Pixley, R. F., Mann, F., Glavish, H. F.: Nucl. Phys. A **160**, 222 (1971)
40. Gückel, F. A., Fick, D.: to be published
41. McNeill, K. G.: Phil. Mag. **46**, 800 (1955)
42. Duder, J. C., Glavish, H. F., Ratcliff, R.: Proceedings of the Third International Symposium on Polarization Phenomena in Nuclear Reactions, p. 459, University of Wisconsin Press 1971
43. Yu, D. U. L.: Progr. Theoret. Phys. (Kyoto) **36**, 734 (1966)
44. Handbook of Mathematical Functions, ed. by Abramowitz, M., Stegum, Irene, A.: NBS Applied Mathematics Serie 55, Washington 1966
45. Lane, A., Thomas, R.: Rev. Mod. Phys. **30**, 257 (1958)
46. Boersma, H. J.: Thesis Free University Amsterdam, 1963
47. Jackson, J. D., Blatt, J. M.: Rev. Mod. Phys. **22**, 77 (1950)

D. Fick
Ursula Weiss
Max-Planck-Institut für Kernphysik
Heidelberg
D-6900 Heidelberg 1
Postfach 1248
Federal Republic of Germany